WUSEAS-2003-50

On Greedy Geographic Routing Algorithms in Sensing-Covered Networks

Authors: Xing, Guoliang; Lu, Chenyang; Pless, Robert; Huang, Qingfeng

July 8, 2003

Abstract: This paper presents a theoretical analysis of greedy geographic routing protocols on a common class of wireless sensor networks that must provide sensing coverage over a geographic area. Contrary to well known results on random networks, we prove that the Greedy Geographic Forwarding and our new greedy protocol always succeed in any sensing covered network when the communication range is at least twice the sensing range. Furthermore, we derive the analytic upper bound for the network dilation of sensing covered networks and quantify its relationship with the ratio between communication range and sensing range. Simulations show that, when the ratio between communication range and sensing range reaches 4.5, the studied greedy routing protocols can find network paths whose hop count on a sensing covered network approaches 1.5 times that of an ideal network. These results provide several important insights into the design of sensor networks. Simple greedy geographic routing protocols are `good

On Greedy Geographic Routing Algorithms in Sensing-Covered Networks

Guoliang Xing, Chenyang Lu, Robert Pless
{xing,lu,pless}@cse.wustl.edu
Department of Computer Science and Engineering
Washington University
St. Louis, MO 63130, USA

Qingfeng Huang
qhuang@parc.com
Palo Alto Research Center (PARC) Inc
3333 Coyote Hill Road, Palo Alto, CA 94304, USA

Abstract

*Greedy geographic routing is attractive in wireless sensor networks due to its efficiency and scalability. However, greedy geographic routing may incur long routing paths or even fail due to routing voids on random network topologies. We study greedy geographic routing in an important class of wireless sensor networks (*e.g.*, surveillance or object tracking systems) that provide sensing coverage over a geographic area. Our geometric analysis and simulation results demonstrate that existing greedy geographic routing algorithms can successfully find short routing paths based on local states in sensing-covered networks. In particular, we derive theoretical upper bounds on the network dilation of sensing-covered networks under greedy geographic routing algorithms. Furthermore, we propose a new greedy geographic routing algorithm called Bounded Voronoi Greedy Forwarding (BVGF) which allows sensing-covered networks to achieve an asymptotic network dilation lower than* 4.62 *as long as the communication range is at least twice the sensing range. Our results show that simple greedy geographic routing is an effective routing scheme in many sensing-covered networks.*

1. Introduction

Wireless sensor networks represent a new type of ad hoc networks that integrate sensing, processing, and wireless communication in a distributed system. While sensor networks have many similarities with traditional ad hoc networks such as those comprised of laptops, they also face new requirements introduced by their distributed sensing applications. In particular, many critical applications (e.g., distributed detection [32], distributed tracking and classification [19]) of sensor networks introduce the fundamental requirement of *sensing coverage* that does not exist in traditional ad hoc networks. In a sensing-covered network, every point in a geographic area of interest must be within the sensing range of at least one sensor.

The problem of providing sensing coverage has received significant attention. Several algorithms [5,7,23, 24] were presented to achieve sensing coverage when a sensor network is deployed. Other projects [31, 33, 35] developed online energy conservation protocols that dynamically maintain sensing coverage using only a subset of nodes.

Complimentary to existing research on coverage provisioning and geographic routing on random network topologies, we study the impacts of sensing coverage on the performance of *greedy geographic routing* in wireless sensor networks.

Geographic routing is a suitable routing scheme in sensor networks. Unlike IP networks, communication on sensor networks often directly use physical locations as addresses. For example, instead of querying a sensor with a particular ID, a user often queries a geographic region. The identities of sensors that happen to be located in that region are not important. Any node in that region that receives the query may participate in data aggregation and reports the result back the user. Due to this location-centric communication paradigm of sensor networks, geographic rout-

ing can be performed without incurring the overhead of location directory services [20]. Furthermore, geographic routing algorithms make efficient routing decisions based on local states (*e.g.*, locations of one-hop neighbors). This localized nature enables geographic routing to scale well in large distributed micro-sensing applications.

As the simplest form of geographic routing, greedy geographic routing is particularly attractive in sensor networks. In this paper, greedy geographic routing refers to a simple routing scheme in which a routing node always forwards a packet to the neighbor that has the shortest distance[1] to the destination. Due to their low processing and memory cost, greedy geographic routing algorithms can be easily implemented on resource constrained sensor network platforms. However, earlier research has shown that greedy geographic routing can incur long routing paths or even fail due to routing voids on random network topologies. In this paper, we present new geometric analysis and simulation results that demonstrate greedy geographic routing is a viable and effective routing scheme in sensing-covered networks. Specifically, the key results in this paper include the following:

- First, we establish a constant upper bound on the network dilation of sensing-covered networks based on Delaunay Triangulations in Section 4.
- We then derive a new upper bound on network dilation for sensor networks under two existing greedy geographic routing algorithms in Section 5. This bound monotonically decreases as the network's range ratio (the communication range divided by the sensing range) increases.
- We also propose a new greedy geographic routing algorithm called Bounded Voronoi Greedy Forwarding (BVGF) that achieves a lower network dilation than two existing greedy geographic routing algorithms (see Section 6).
- Finally, our analytic results and simulations (see Section 8) demonstrated that both BVGF and existing greedy geographic routing algorithms can successfully find short routing paths in sensing-covered networks with high range ratios.

2. Related Work

Routing in ad hoc wireless (sensor) networks has been studied extensively in the past decade. The most relevant work includes various geographic routing algorithms [3, 4, 17, 22, 26, 29, 30]. Existing geographic routing algorithms switch between *greedy* mode and *recovery* mode depending on the network topology. In greedy mode, GPSR (Greedy Perimeter Stateless Routing) [17] and Cartesian routing [13] choose the neighbor closest to the destination as the next hop while MFR (Most Forward within Radius) [30] prefers the neighbor with shortest projected distance (on the straight line joining the current node and the destination) to the destination. In this paper, we refer to these two greedy routing schemes as *greedy forwarding* (GF). Although GF is very efficient, it may fail if a node encounters local minima, which occurs when it cannot find a "better" neighbor than itself due to the *routing voids* on the network topology. Previous studies found routing voids are prevalent in ad hoc networks, and hence it is important for geographic routing algorithms to recover when a packet reaches a routing void. To recover from local minima, GPSR [17] and GOAFR [18] route a packet around the faces of a planar subgraph extracted from the original network, while limited flooding is used in [29] to circumvent the routing void. Unfortunately, the recovery mode inevitably introduces additional overhead and complexity to geographic routing algorithms.

Analysis on (network and Euclidean) stretch factors of specific geometric topologies has been studied in the context of wireless networks. The recovery algorithm in GPSR [17] routes packets around the faces of one of two planar subgraphs, namely *Relative Neighborhood Graph* (RNG) and *Gabriel Graph* (GG), to escape from routing voids. However GG and RNG are not good spanners of the original graph [12], *i.e.*, two nodes that are few hops away in the original network might be very far apart in GG and RNG.

The *Delaunay Triangulation* (DT) has been shown to be a good spanner with a constant stretch factor [6, 10, 16]. However, the DT of a random network topology may contain arbitrarily long edges which exceed limited wireless transmission range. To enable the local routing algorithms to leverage on the good spanning property of DT, [14, 21] proposed two distributed algorithms for constructing local approximations of the DT. Interestingly, these local approximations to DT are also good spanners with the same constant stretch factor as DT. However, finding the routing path with bounded length in DT requires global topology information [10]. Parallel Voronoi Routing(PVR) [2] algorithm deals with this problem by exploring the parallel routes which may have bounded lengths. Unlike the existing works that assume arbitrary node distribution, our work focuses on the greedy geographic routing on

1 Different definitions of distance (*e.g.*, Euclidean distance or projected distance on the straight line toward the destination) may be adopted by different algorithms.

sensing-covered topologies.

3. Preliminaries

In this section, we introduce a set of assumptions and definitions used throughout the rest of this paper.

3.1. Assumptions

We assume every node integrates sensors, processing units, and a wireless interface. All nodes are located in a two dimensional space. Every node has the same sensing range R_s. For a node located at point p, we use circle $C(p, R_s)$ that is centered at point p and has radius R_s to represent the *sensing circle* of the node. A node can *cover* any point inside its sensing circle. We assume that a node does not cover points *on* its sensing circle. While this assumption has little impact on the performance of a sensor network in practice, it simplifies our theoretical analysis. A network deployed in a convex region A is *covered* if any point in A is covered by at least one node. Any two nodes u and v can directly communicate with each other if and only if $|uv| \leq R_c$, where $|uv|$ is the Euclidean distance between u and v, and R_c is the communication range of the wireless network. The graph $G(V, E)$ is the *communication graph* of a set of nodes V, where each node is represented by a vertex in V, and edge $(u, v) \in E$ if and only if $|uv| \leq R_c$. For simplicity, we also use $G(V, E)$ to represent the sensor network whose communication graph is $G(V, E)$.

3.2. Double Range Property

The ratio between the communication range, R_c, and the sensing range, R_s, has a significant impact on the routing quality of a sensing-covered network. In this paper, we call R_c/R_s the *range ratio*. Intuitively, a sensing-covered network with a larger range ratio has a denser communication graph and hence better routing quality.

In practice, both communication and sensing ranges are highly dependent on the system platform, the application, and the environment. The communication range of a wireless network interface depends on the property of radio (*e.g.*, transmission power, baseband/wide-band, and antenna) and the environment (*e.g.*, indoor or outdoor) [36]. The outdoor communication ranges of several wireless (sensor) network interfaces are listed in Table 1. This data was obtained from the product specifications from their vendors [8, 9, 27, 28][2].

The sensing range of a sensor network depends on the sensor modality, sensor design, and the requirements of specific sensing applications. The sensing range has a significant impact on the performance of a sensing application and is usually determined empirically to satisfy the Signal-to-Noise Ratio (SNR) required by the application. For example, the empirical results in [11] showed that the performance of target classification degrades quickly with the distance between a sensor and a target. In their real-world experiments on sGate [27], a sensor platform from Sensoria Corp., different types of military vehicles drove through the sensor deployment region and the types of the vehicles were identified based on the acoustic measurements. The experimental results showed that the probability of correct vehicle classification decreases quickly with the sensor-target distance, and drops below 50% when the sensor-target distance exceeds $100m$. Hence the effective sensing range is much shorter than $100m$. The experiments for a similar application [15] showed that the sensing range of seismic sensors is about $50m$.

Clearly, the range ratio can vary across a wide range for different sensor networks due to the heterogeneity of such systems. As a starting point for the analysis, in this paper we focus on those networks with the *double range property*, *i.e.*, $R_c/R_s \geq 2$. This assumption is motivated by the geometric analysis in [33], which proved that a sensing-covered network is always connected if it has the double range property. Since network connectivity is necessary for any routing algorithm to find a routing path, it is reasonable to assume the double-range property as a starting point.

Empirical experiences have shown that the double range property is applicable to a number of representative sensing applications. For example, the aforementioned sGate-based network used for target classification [11] has a sensing range $R_s < 100m$, and communication range $R_c = 1640ft$ $(547m)$ (as shown in Table 1), which corresponds to a range ratio $R_c/R_s > 5.47$. The double range property will also hold if the seismic sensor used in [15] is combined with a wireless network interface that has a communication range $R_c \geq 100m$.

All results and analyses in the rest of this paper assume a sensor network has the double property unless otherwise stated.

3.3. Metrics

The performance of a routing algorithm can be characterized by the *network length* (*i.e.*, hop count) and

2 The empirical study in [36] shows that the effective communication range of Mica1 varies with different environments and usually is shorter than $30m$.

Platforms	Berkeley Mote (Mica 1)	Berkeley Mote (Mica 2)	Sensoria SGate	802.11b (SonicWall)
R_c (ft)	100	1000	1640	$1200 \sim 2320$

Table 1: The Communication Ranges of Wireless Network Platforms

Euclidean length (*i.e.*, the sum of the Euclidean distance of each hop) of the routing paths it finds. Note the path with shortest network length may be different from the path with shortest Euclidean length. In this paper, we focus more on the network length. Network length has a significant impact on the delay and throughput of multi-hop ad hoc networks. A routing algorithm that can find the paths with short Euclidean length may potentially reduce the network energy consumption by controlling the transmission power of the wireless nodes [25, 34].

The performance a routing algorithm is inherently affected by the path quality of the underlying networks. *Stretch factor* [12] is an important metric for comparing the path quality between two graphs. Let $\tau_G(u, v)$ and $d_G(u, v)$ represent the shortest network and Euclidean length between nodes u and v in graph $G(V, E)$, respectively. A subgraph $H(V, E')$, where $E' \subseteq E$, is a *network t-spanner* of graph $G(V, E)$ if

$$\forall\ u, v \in V, \tau_H(u, v) \leq t \cdot \tau_G(u, v)$$

Similarly, $H(V, E')$ is an *Euclidean t-spanner* of graph $G(V, E)$ if

$$\forall\ u, v \in V, d_H(u, v) \leq t \cdot d_G(u, v)$$

where t is called *network (Euclidean) stretch factor* of the spanner $H(V, E')$.

In this paper, we use *dilation* to represent the stretch factor of the wireless network $G(V, E)$ relative to an *ideal* wireless network in which there exist a path with network length $\left\lceil \frac{|uv|}{R_c} \right\rceil$ and a path with Euclidean length $|uv|$ for any two nodes u and v. The network and Euclidean dilations[3] (denoted by D_n and D_e, respectively) of network $G(V, E)$ are defined as follows:

$$D_n = \max_{u,v \in V} \frac{\tau_G(u, v)}{\left\lceil \frac{|uv|}{R_c} \right\rceil} \quad (1)$$

$$D_e = \max_{u,v \in V} \frac{d_G(u, v)}{|uv|} \quad (2)$$

Clearly, the network (Euclidean) dilation of a wireless network is an upper bound of the network (Euclidean) stretch factor relative to *any* possible wireless network composed of the same set of nodes.

Asymptotic network dilation (denoted by $\tilde{D_n}$) is the value that the network dilation converges to when the network length approaches infinity. Asymptotic network dilation is useful in characterizing the path quality of a large-scale wireless network.

We say $D_n(R)$ is the *network dilation of the wireless network* $G(V, E)$ *under routing algorithm* R, (or *network dilation of* R for abbreviation), if $\tau_G(u, v)$ in (1) represents the network length of the routing path between nodes u and v chosen by R. The network dilation of a routing algorithm characterizes the performance of the algorithm relative to the *ideal* case in which the path between any two nodes u and v has $\left\lceil \frac{|uv|}{R_c} \right\rceil$ hops. The Euclidean dilation of the routing algorithm R is defined similarly.

4. Dilation Analysis Based on DT

In this section we study the dilation property of sensing-covered networks based on Delaunay Triangulations (DT). We first study the DT of sensing-covered networks and prove that the DT of a sensing-covered network is a subgraph of the communication graph, when the double-range property holds. We then quantify the Euclidean and network dilations of sensing-covered networks.

4.1. Voronoi Diagram and Delaunay Triangulation

Voronoi diagram is one of the most fundamental structures in computational geometry and has found applications in a variety of fields [1]. For a set of n nodes V in 2D space, the Voronoi diagram of V is the partition of the plane into n *Voronoi regions*, one for each node in V. The Voronoi region of node i ($i \in V$) is denoted by *Vor(i)*. Fig. 1 shows a Voronoi diagram of a set of nodes. A point in the plane lies in *Vor(i)* if and only if i is the closest node to the point. The boundary between two contiguous Voronoi regions is called a *Voronoi edge*. A Voronoi edge is on the perpendicular bisector of the segment connecting two adjacent nodes. A *Voronoi vertex* is the intersection of Voronoi edges. As shown in Fig. 1, point p is a Voronoi vertex of three contiguous Voronoi regions: *Vor(u)*, *Vor(v)* and

3 Euclidean dilation has been widely used in graph theory to characterize the quality of a graph [12].

Vor(w). We assume that all nodes are in *general positions* (*i.e.*, no four nodes are co-circular).

In the dual graph of Voronoi diagram, Delaunay Triangulation (denoted by $DT(V)$), there is an edge between nodes u and v in $DT(V)$ if and only if the Voronoi regions of nodes u and v share a boundary. $DT(V)$ consists of *Delaunay triangles*. Fig. 1 shows a Delaunay triangle uvw. $DT(V)$ is planar, *i.e.*, no two edges cross. It has been shown in [10] that the Delaunay Triangulation of a set of nodes is a good Euclidean spanner of the complete Euclidean graph composed of the same set of nodes. The upper bound of the Euclidean stretch factor is $\frac{1+\sqrt{5}}{2}\pi$ [10]. A tighter bound on the stretch factor, $\frac{4\sqrt{3}}{9}\pi \approx 2.42$, is proved in [16].

4.2. Dilation Property

In this section, we investigate the Euclidean and network dilations of sensing-covered networks. We first study the properties of Voronoi diagrams and DT in sensing-covered networks. These results lead to bounded dilations of such networks.

In a sensing-covered network deployed in a convex region A, the Voronoi region of a node located at the vicinity of A's boundary may exceed the boundary of A or even be unbounded. In the rest of this paper, we only consider the partial Voronoi diagram that is bounded by the deployment region A and the corresponding dual graph. As illustrated in Fig. 1, the Voronoi region of any node in this partial Voronoi diagram is contained in the region A. Consequently, the dual graph of this partial Voronoi diagram is a partial DT that does not contain the edges between any two nodes whose Voronoi regions (of the original Voronoi diagram) joins outside A.

In a sensing-covered convex region, any point is covered by the node closest to it. This simple observation results in the the following Lemma.

Lemma 1 (Coverage Lemma). *A convex region A is covered by a set of nodes V if and only if each node can cover its Voronoi region (including the bounary).*

Proof. The nodes partition convex region A into a number of Voronoi regions in the Voronoi diagram. Clearly, if each Voronoi region (including the boundary) is covered by the node within it, region A is sensing-covered.

On the other hand, if region A is covered, any point in region A must be covered by the *closest* node(s) to it. In the Voronoi diagram, all the points in a Voronoi region share the same closest node. Thus every node can cover all the points in its Voronoi region. Any point on the boundary of two Voronoi regions *Vor*(i) and *Vor*(j) has the same distance from i and j and is covered by both of them. □

According to Lemma 1, every Voronoi region *Vor(u)* in a sensing-covered network is contained in the sensing circle of u. This property results in the following Lemma.

Lemma 2. *In a sensing-covered network $G(V, E)$ deployed in region A, the Delaunay Triangulation of the nodes is a subgraph of the communication graph,* i.e., *$DT(V) \subseteq G(V, E)$. Furthermore, any DT edge is shorter than $2R_s$.*

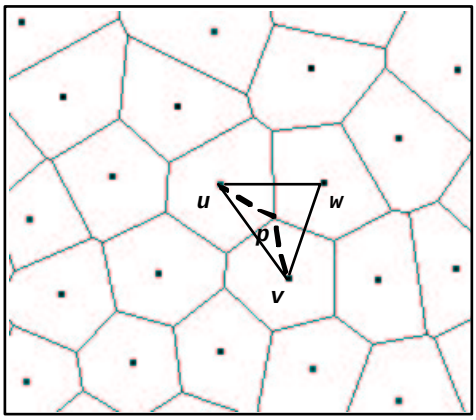

Figure 1: The Voronoi Diagram of a Sensing-covered Network

Proof. It is clear that the two graphs $DT(V)$ and $G(V, E)$ share the same set of vertices. We now show that any DT edge between u and v is also an edge in $G(V, E)$. As illustrated in Fig. 1, the Voronoi vertex p is the intersection of three contiguous Voronoi regions, *Vor(u)*, *Vor(v)* and *Vor(w)*. From Lemma 1, p is covered by u, v and w. Hence $|pu|$, $|pv|$ and $|pw|$ are all less than R_s. Thus from triangle inequality,

$$|uv| \leq |up| + |pv| < 2R_s$$

From the double range property, we have $|uv| < R_c$. Therefore uv is an edge in the communication graph $G(V, E)$. □

Since the communication graph of a sensing-covered network contains the DT of the nodes, the dilation property of a sensing-covered network is at least as good as DT.

Theorem 1. *A sensing-covered network $G(V, E)$ has a Euclidean dilation $\frac{4\sqrt{3}}{9}\pi$.* i.e., *$\forall\, u, v \in V, d_G(u, v) \leq \frac{4\sqrt{3}}{9}\pi|uv|$.*

Proof. As proved in [16], the upper bound on the stretch factor of DT is $\frac{4\sqrt{3}}{9}\pi$. From Lemma 2, $DT(V) \subseteq G(V, E)$, thus we have

$$\forall\ u, v \in V, d_G(u, v) \leq d_{DT}(u, v) \leq \frac{4\sqrt{3}}{9}\pi|uv| \qquad \square$$

In addition to the competitive Euclidean dilation shown by Theorem 1, we next show that a sensing-covered network also has a good network dilation.

Theorem 2. *In a sensing-covered network $G(V, E)$, the network length of the shortest path between node u and v satisfies*

$$\tau_G(u, v) \leq \left\lfloor \frac{8\pi\sqrt{3}}{9} \cdot \frac{|uv|}{R_c} \right\rfloor + 1 \qquad (3)$$

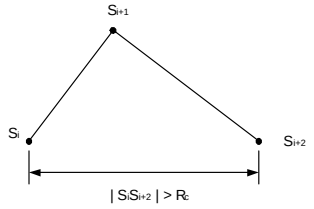

Figure 2: Three Consecutive Nodes on Path Π

Proof. Clearly the theorem holds if the nodes u and v are adjacent in $G(V, E)$. Now we consider the case where the network length between u and v is at least 2. Let Π represent the path in $G(V, E)$ that has the shortest Euclidean length among all paths between nodes u and v. Let N be the network length of path Π. Consider three consecutive nodes s_i, s_{i+1} and s_{i+2} on Π, as illustrated in Fig. 2. Clearly, there is no edge between s_i and s_{i+2} in $G(V, E)$ because, otherwise, choosing node s_{i+2} as the next hop of node s_i results in a path with shorter Euclidean length than Π, which contradicts the assumption that Π is the path with the shortest Euclidean length between u and v in term of Euclidean distance. Hence the Euclidean distance between nodes s_i and s_{i+2} is longer than R_c. From triangle inequality, we have

$$|s_i s_{i+1}| + |s_{i+1} s_{i+2}| > |s_i s_{i+2}| > R_c$$

Summing the above inequality over consecutive hops on the path, we have:

$$R_c \left\lfloor \frac{N}{2} \right\rfloor < d_G(u, v) \qquad (4)$$

From Theorem 1, we have

$$d_G(u, v) \leq \frac{4\sqrt{3}\pi R_c}{9} \frac{|uv|}{R_c} \qquad (5)$$

From (4) and (5), the shortest network length between nodes i and j satisfies:

$$\tau_G(u, v) \leq N \leq \left\lfloor \frac{8\pi\sqrt{3}}{9} \cdot \frac{|uv|}{R_c} \right\rfloor + 1 \qquad \square$$

From Theorem 2, we can obtain the *asymptotic* bound on the network dilation of sensing-covered networks by ignoring the rounding and constant term 1 in (3).

Corollary 1. *The asymptotic network dilation of sensing-covered networks is $\frac{8\sqrt{3}\pi}{9}$.*

Theorem 1 and Corollary 1 show that the sensing-covered networks have good Euclidean and network dilation properties.

We note that the analysis in this section only considers the DT subgraph of the communication graph and ignores any communication edge that is not a DT edge. When R_c/R_s is large, a DT edge in a sensing-covered network can be significantly shorter than R_c, and the dilation bounds based DT can be very conservative. In the following sections we will show that significantly tighter dilation bounds on sensing-covered networks are achieved by greedy routing algorithms such as GF when R_c/R_s becomes higher.

5. Greedy Forwarding

Greedy forwarding (GF) is an efficient, localized ad hoc routing scheme employed in many existing geographic routing algorithms [13, 17, 30]. Under GF a node makes routing decisions only based on the locations of its (one-hop) neighbors, thereby avoiding the overhead of maintaining global topology information. In each step a node forwards a packet to the neighbor with the shortest Euclidean distance to the destination [13, 17]. An alternative greedy forwarding scheme [30] chooses the neighbor with the shortest projected distance to the destination on the straight line joining the current node and the destination, where the projected distance between two points i and j on line AB is defined as the Euclidean distance between the projections of i and j on AB.

However, a routing node might encounter a *routing void* when it cannot find a neighbor that is closer (in term of Euclidean or projected distance) to the destination than itself. In such a case, the routing node must drop the packet or enter a more complex recovery modes [17, 18, 29] to route the packet around the routing void. In this section we prove GF always succeeds in

sensing-covered networks when the double-range property is satisfied. We further derive the upper bound on the network dilation of sensing-covered networks under GF.

Theorem 3. *In a sensing-covered network, GF can always find a routing path between any two nodes. Furthermore, in each step (other than the last step arriving at the destination), a node can always find a next-hop node that is more than $R_c - 2R_s$ closer (in terms of both Euclidean and projected distance) to the destination than itself.*

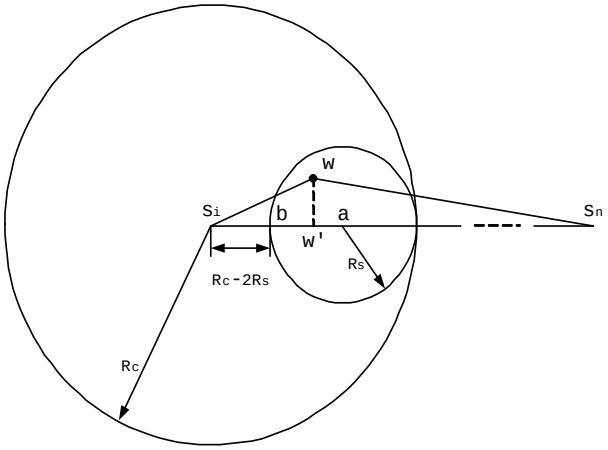

Figure 3: GF Always Finds a Next-hop Node

Proof. Let s_n be the destination, and s_i be either the source or an intermediate node on the GF routing path, as shown in Fig. 3. If $|s_i s_n| \leq R_c$, the destination is reached in one hop. If $|s_i s_n| > R_c$, we find point a on the line segment $\overline{s_i s_n}$ such that $|s_i a| = R_c - R_s$. Since $R_c \geq 2R_s$, point a must be outside of the sensing circle of s_i. Since a is covered, there must be at least one node, say w, inside the circle $C(a, R_s)$.

We now prove the progress toward destination s_n (in terms of both Euclidean and projected distance) is more than $R_c - 2R_s$ by choosing w as the next hop of s_i. Let point b be the intersection between line segment $\overline{s_i s_n}$ and circle $C(a, R_s)$ that is closest to s_i. Since circle $C(a, R_s)$ is internally tangent with the communication circle of node s_i, $|s_i b| = R_c - 2R_s$. Clearly, the maximal distance between point s_n and any point on or inside circle $C(a, R_s)$ is $|s_n b|$. Since point w is inside $C(a, R_s)$, $|s_n w| < |s_n b|$. Suppose w' is the projection of node w on line segment $\overline{s_i s_n}$. We have:

$$\begin{aligned} |s_n s_i| - |s_n w'| \geq |s_n s_i| - |s_n w| &> |s_n s_i| - |s_n b| \\ &= |s_i b| \\ &= R_c - 2R_s \\ &\geq 0 \end{aligned} \quad (6)$$

From above relation, we can see that both the projected distance and Euclidean distance between node w and destination s_n is more than $R_c - 2R_s$ shorter than $|s_i s_n|$. This leads to the conclusion that GF can choose a next hop that is more than $R_c - 2R_s$ closer (in terms of both projected and Euclidean distance) to the destination than the current node. Since this holds for every step (other than the last step arriving at the destination), GF always can find a routing path between any two nodes. □

Theorem 3 establishes that the progress toward the destination in each step of a GF routing path is lower-bounded by $R_c - 2R_s$. Therefore, the network length of a GF routing path between a source and a destination is upper-bounded.

Theorem 4. *In a sensing-covered network, GF can always find a routing path between source u and destination v no longer than $\left\lfloor \frac{|uv|}{R_c - 2R_s} \right\rfloor + 1$ hops.*

Proof. Let N be the network length of the GF routing path between u and v. The nodes on the path are $s_0(u)$,$s_1 \cdots s_{n-1}$,$s_n(v)$. From Theorem 3, we have

$$\begin{aligned} |s_0 s_n| - |s_1 s_n| &> R_c - 2R_s \\ |s_1 s_n| - |s_2 s_n| &> R_c - 2R_s \\ &\vdots \\ |s_{n-2} s_n| - |s_{n-1} s_n| &> R_c - 2R_s \end{aligned}$$

Summing all the equations above, we have:

$$|s_0 s_n| - |s_{n-1} s_n| > (N-1)(R_c - 2R_s)$$

Given $|s_0 s_n| = |uv|$, we have:

$$\begin{aligned} N &< \frac{|uv| - |s_{n-1} s_n|}{R_c - 2R_s} + 1 \\ &< \frac{|uv|}{R_c - 2R_s} + 1 \end{aligned} \quad (7)$$

Hence $N \leq \left\lfloor \frac{|uv|}{R_c - 2R_s} \right\rfloor + 1$ □

From Theorem 4 and (1), the network dilation of a sensing-covered network $G(V, E)$ under GF satisfies:

$$D_n(GF) \leq \max_{u,v \in V} \left(\frac{\left\lfloor \frac{|uv|}{R_c - 2R_s} \right\rfloor + 1}{\left\lceil \frac{|uv|}{R_c} \right\rceil} \right) \quad (8)$$

The *asymptotic* bound on network dilation of sensing-covered networks under GF can be computed by ignoring the rounding and the constant term 1 in (8).

Corollary 2. *The asymptotic network dilation of sensing-covered networks under GF satisfies*

$$\tilde{D}_n(GF) \leq \frac{R_c}{R_c - 2R_s} \tag{9}$$

From (9), the upper bound on the network dilation of sensing-covered networks under GF monotonically decreases when R_c/R_s increases. The upper bound becomes lower than 2 when $R_c/R_s > 4$, and approaches 1 when R_c/R_s becomes very large. This result confirms our intuition that a sensing-covered network approaches an ideal network in terms of network length when the communication range is significantly longer than the sensing range.

However, the GF bound in (9) increases quickly to infinity when R_c/R_s approaches 2. In the proof of Theorem 3, when R_c approaches $2R_s$, a forwarding node s_i may be infinitely close to the intersection point between $C(a, R_s)$ and $\overline{s_i s_n}$. Consequently, s_i may choose a neighbor inside $C(a, R_s)$ that makes infinitely small progress toward the destination resulting in a long routing path. It has been shown in [14] that the network length of a GF routing path between source u and destination v is bounded by $O((\frac{|uv|}{R_c})^2)$. From (1), we can see that this result cannot lead to a constant upper bound on the network dilation for a given range ratio. Whether GF has a tighter analytical network dilation bound when R_c/R_s is close to two is an open research question left for future work.

6. Bounded Voronoi Greedy Forwarding (BVGF)

From Sections 5, we note that although GF has satisfactory network dilation bound on sensing-covered networks when $R_c/R_s \gg 2$, the bound becomes very large when R_c/R_s is close to two. In contrast, the analysis based on Voronoi diagram leads to a satisfactory bound when R_c/R_s is close to two, but this bound becomes conservative when $R_c/R_s \gg 2$. These results motivate us to develop a new routing algorithm, Bounded Voronoi Greedy Forwarding (BVGF), that has satisfactory analytical dilation bound for any $R_c/R_s > 2$ by combining GF and Voronoi diagram.

6.1. The BVGF Algorithm

Similar to GF, BVGF is a localized algorithm that makes greedy routing decisions based on one-hop neighbor locations. When node i needs to forward a packet, a neighbor j is eligible as the next hop only if the line segment joining the source and the destination of the packet intersects *Vor(j)* or coincides with one of the boundaries of *Vor(j)*. BVGF chooses as the next hop the neighbor that has the shortest Euclidean distance to the destination among all eligible neighbors. When there are multiple eligible neighbors that are closest to the destination, the routing node randomly chooses one as the next hop. Fig. 4 illustrates four consecutive nodes ($s_i \sim s_{i+3}$) on the BVGF routing path from source u to destination v. The communication circle of each node is also shown in the figure. We can see that a node's next hop in a routing path might not be adjacent with it in the Voronoi diagram (*e.g.*, node s_i does not share a Voronoi edge with node s_{i+1}). When $R_c \gg R_s$, this greedy forwarding scheme allows BVGF to achieve a tighter dilation bound than the DT bound that only considers DT edges and does not vary with the range ratio.

The key difference between GF and BVGF is that BVGF only considers the neighbors whose Voronoi regions intersect the line joining the source and the destination. As we will show later in this section, this feature allows BVGF to have a tighter upper-bound on network dilation in sensing-covered networks.

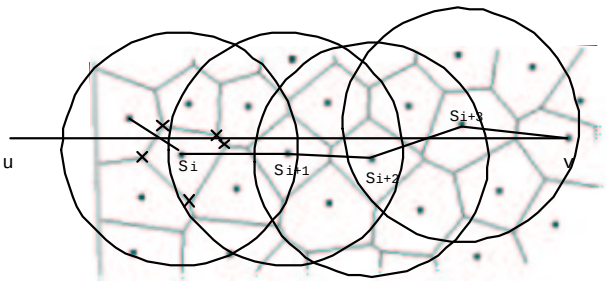

Figure 4: A Routing Path of BVGF

In BVGF, each node maintains a neighborhood table. For each one-hop neighbor j, the neighborhood table includes $j's$ location and the locations of the vertices of *Vor*(j). For example, as illustrated in Fig. 4, for one-hop neighbor s_i, node s_{i+1} includes in its neighborhood table the locations of s_i and the vertices of *Vor*(s_i) (each vertex is denoted by a cross in the figure). To maintain the neighborhood table, each node periodically broadcasts a beacon message that includes its own location as well as the locations of the vertices of its Voronoi region. Note each node can compute its own Voronoi vertices based on its neighbor locations because all Voronoi neighbors are within its communi-

cation range (as proved in Lemma 2).

Assume the number of neighbors within a node's communication range is bounded by $O(n)$. The complexity incured by a node to compute the Voronoi diagram of all its one-hop neighbors is $O(n \log n)$ [1]. Since the number of vertices of the Voronoi region of a node is bounded by $O(n)$ [1], the total storage complexity of a node's neighborhood table is $O(n^2)$.

6.2. Network Dilation of BVGF

In this section, we analyze the network dilation of BVGF. We first prove that BVGF can always find a routing path between any two nodes in a sensing-covered network (Theorem 5). We next show that a BVGF routing path always lies in a *Voronoi forwarding rectangle*. We then derive the lower bound on the projected progress in every step of a BVGF routing path (Lemma 4). Since this lower bound is not tight when R_c/R_s is close to two, we derive the lower bound on the projected progress in two and four consecutive steps in a BVGF routing path (Lemmas 7 and 8) based on the *non-adjacent advancing property*. Finally we establish the asymptotic bounds of the network dilation of sensing-covered networks under BVGF in Theorem 7.

In the rest of this section, to simplify our discussion on the routing path from source u to destination v, we assume node u is the origin and the straight line joining u and v is the *x-axis*. The *Voronoi forwarding rectangle* of nodes u and v refers to the rectangle defined by the points $(0, R_s)$, $(0, -R_s)$, $(|uv|, -R_s)$ and $(|uv|, R_s)$. Let $x(a)$ and $y(a)$ denote the x-coordinate and y-coordinate of a point a, respectively. The projected progress $pp(a, b)$ from node a to node b is defined as the difference between their x-coordinates, *i.e.*, $pp(a, b) = x(b) - x(a)$.

Theorem 5. *In a sensing-covered network, BVGF can always successfully find a routing path between any two nodes. Furthermore, the projected progress in each step of a BVGF routing path is positive.*

Proof. As illustrated in Fig. 5, node s_i is an intermediate node on the BVGF routing path from source u to destination v. *x-axis* intersects $Vor(s_i)$ or coincides with one of the boundaries of $Vor(s_i)$. Let point p be the intersection between $Vor(s_i)$ and the *x-axis* that is closer to v (if *x-axis* coincides with one of the boundaries of $Vor(s_i)$, we choose the vertex of $Vor(s_i)$ that is cloest to v as point p). There must exist a node w such that $Vor(s_i)$ and $Vor(w)$ share the Voronoi edge that hosts p and intersects the *x-axis*. The straight line (denoted as dotted line in Fig. 5) where the Vornoi

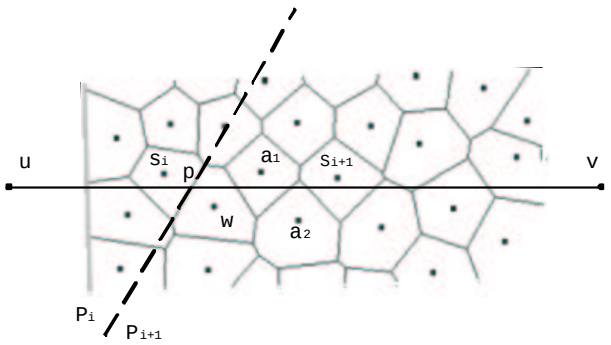

Figure 5: BVGF Always Finds a Next-hop Node

edge lies on defines two half-planes P_i and P_{i+1}, and $s_i \in P_i, w \in P_{i+1}$. From the definition of Voronoi diagram, any point in half-plane P_{i+1} has a shorter distance to w than to s_i. Since $v \in P_{i+1}$, $|wv| < |s_i v|$. In addition, since $|s_i w| < 2R_s \leq R_c$ (see Lemma 2) and line segment $\overline{uv}$ intersects $Vor(w)$ (or coincides with one of the boundaries of $Vor(w)$), w is eligible to be the next hop of s_i. That is, s_i can find at least one neighbor (w) closer to the destination. This holds for every node other than the destination and hence BVGF can always find a routing path between the source and the destination.

We now prove the projected progress in each step of a BVGF routing path is positive. We discuss two cases. 1) If s_i chooses w as the next hop on the BVGF routing path, from the definition of Voronoi diagram, s_i and w lies to the left and the right of the perpendicular bisector of line segment $\overline{s_i w}$, respectively. Therefore, $x(s_i) < x(p) < x(w)$ and hence the projected progress between s_i and w is positive. 2) If s_i chooses node s_{i+1} (which is different from w) as the next hop, we can construct a consecutive path (along the *x-axis*) consisting of the nodes s_i, $a_0(w)$, $a_1 \cdots a_m$, s_{i+1} such that any two adjacent nodes on the path share a Voronoi edge that intersects the *x-axis*, as illustrated in Fig. 5. Similarly to case 1), we can prove:

$$x(s_i) < x(a_0) < \cdots < x(a_m) < x(s_{i+1})$$

Hence the projected progress between the consecutive nodes s_i and s_{i+1} on the BVGF routing path is positive.

□

BVGF always forwards a packet to a node whose Voronoi region is intersected by the straight line joining the source and the destination. From Lemma 1, every Voronoi region in a sensing-covered network is within a sensing circle. Therefore, every node on a BVGF routing path lies in a bounded region. Specifically, we have the following Lemma.

Lemma 3. *The BVGF routing path from node u to node v lies in the Voronoi forwarding rectangle of nodes u and v.*

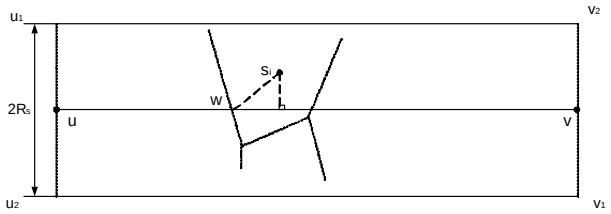

Figure 6: Voronoi Forwarding Rectangle

Proof. As illustrated in Fig. 6, s_i is an intermediate node on the BVGF routing path between u and v. Let point w be one of the intersections between the *x-axis* and *Vor*(s_i) (if *x-axis* coincides with one of the boundaries of *Vor*(s_i), choose a vertex on the boundary as point w). From Lemma 1, node s_i covers point w, and hence $|s_i w| < R_s$. We have $|y(s_i)| \leq |s_i w| < R_s$. Furthermore, from Theorem 5, $0 < |x(s_i)| < |uv|$. Thus, s_i lies in the Voronoi forwarding rectangle of nodes u and v. □

In a sensing-covered network, the greedy nature of BVGF ensures that a node chooses a next hop that has the shortest distance to the destination among all eligible neighbors. On the other hand, according to Lemma 3, the next-hop node must fall in the Voronoi forwarding rectangle. These results allow us to derive a lower bound on the progress of every step in a BVGF routing path.

Lemma 4 (One-step Advance Lemma). *In a sensing-covered network, the projected progress in each step of a BVGF routing path is more than* Δ_1*, where* $\Delta_1 = \max(0, \sqrt{R_c^2 - 2R_cR_s} - R_s)$.

Proof. As illustrated in Fig. 7, s_i is an intermediate node on the BVGF routing path between source u and destination v. Let point s_i' be the projection of s_i on the *x-axis*. From Lemma 3, $s_i s_i' < R_s$. Let point d be the point on the *x-axis* such that $|s_i d| = R_c - R_s$. According to Lemma 1, there must exist a node, w, which covers point d and $d \in$ *Vor(w)*. Clearly w lies in circle $C(d, R_s)$. Since d is on the *x-axis* and $d \in$ *Vor(w)*, *x-axis* intersects *Vor(w)*. Furthermore, since circle $C(d, R_s)$ is internally tangent with the communication circle of node s_i, node w is within the communication range of node s_i. Therefore node s_i can at least choose node w as the next hop. Let c be the intersection between $C(d, R_s)$

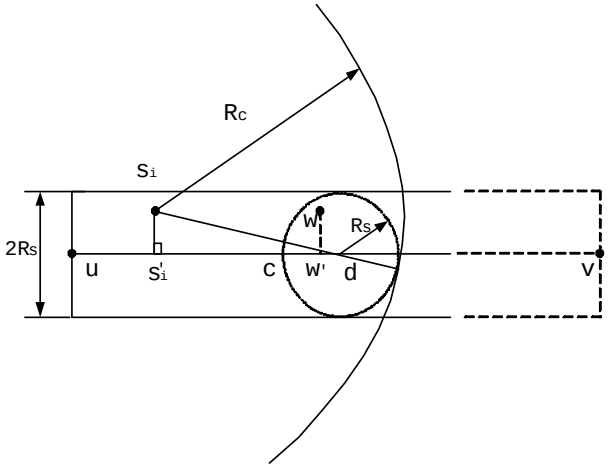

Figure 7: One-step Projected Progress of BVGF

and *x-axis* that is closest to u. Let w' be the projection of w on the *x-axis*. The projected progress between s_i and w is:

$$\begin{aligned} |s_i' w'| &> |s_i' c| \\ &= |s_i' d| - R_s \\ &= \sqrt{|s_i d|^2 - |s_i s_i'|^2} - R_s \\ &> \sqrt{(R_c - R_s)^2 - R_s^2} - R_s \\ &= \sqrt{R_c^2 - 2R_cR_s} - R_s \end{aligned}$$

$|s_i' w'| \leq 0$ whe $R_c/R_s \leq 1 + \sqrt{2}$. From Theorem 5, projected progress made by BVGF in each step is positive. Therefore, the lower bound on the projected progress in each step is $\max(0, \sqrt{R_c^2 - 2R_cR_s} - R_s)$. □

From Lemma 4, we can see that the lower bound on the projected progress between any two nodes in a BVGF routing path approaches zero when $R_c/R_s \leq 1 + \sqrt{2}$. We ask the question whether there is a tighter lower bound in such a case.

Consider two non-adjacent nodes i and j on a BVGF routing path. The Euclidean distance between them must be longer than R_c because otherwise BVGF would have chosen j as the next hop of i which contradicts the assumption that i and j are non-adjacent on the routing path. We refer to this property of BVGF as the *non-adjacent advancing property*. We have the following Lemma (the detailed proof is similar to the proof of Theorem 2 and omitted due to the space limitation) [4].

Lemma 5 (Non-adjacent Advancing Property). *In a sensing-covered network, the Euclidean distance be-*

4 Similarly, GF also can be shown to have this property.

tween any two non-adjacent nodes on a BVGF routing path is longer than R_c.

The non-adjacent advancing property, combined with the fact that a BVGF routing path always lies in the Voronoi forwarding rectangle, leads to the intuition that the projected progress toward the destination made by BVGF in two consecutive steps is lower-bounded. Specifically, we have the following Lemma that establishes a tighter bound on the projected progress of BVGF than Lemma 4 when R_c/R_s is small.

Lemma 6. *In a sensing-covered network, the projected progress between any two non-adjacent nodes i and j on a BVGF routing path is more than:*

$$\begin{array}{ll} \sqrt{R_c^2 - R_s^2} & \text{if } i, j \text{ on the same side of the } x\text{-axis} \\ \sqrt{R_c^2 - 4R_s^2} & \text{if } i, j \text{ on different sides of the } x\text{-axis} \end{array}$$

Proof. Let $s_0(u)$,$s_1 \cdots s_{n-1}$,$s_n(v)$ be the consecutive nodes on the BVGF routing path between source u and destination v. From Lemma 5, $|s_i s_{i+k}| > R_c$ $(k > 1)$. Fig. 8(a) and (b) illustrate the two cases where s_i and s_{i+k} are on the same or different sides of the *x-axis*, respectively. Both s_i and s_{i+k} lie in the Voronoi forwarding rectangle of nodes u and v (dotted box in the figure). When s_i and s_{i+k} are on the same side of the *x-axis*, we have

$$|y(s_{i+k}) - y(s_i)| < R_s$$

The projected progress between s_{i+k} and s_i satisfies:

$$\begin{array}{rcl} x(s_{i+k}) - x(s_i) & = & \sqrt{|s_i s_{i+k}|^2 - (y(s_{i+k}) - y(s_i))^2} \\ & > & \sqrt{R_c^2 - R_s^2} \end{array}$$

Similarly, when s_i and s_{i+k} are on different sides of the *x-axis* as shown in Fig. 8(b), we can prove that the projected progress between them is more than $\sqrt{R_c^2 - 4R_s^2}$. □

From Lemma 6, we can see that the worst-case projected progress in two consecutive steps on a BVGF routing path occurs when the non-adjacent nodes on the two steps are on the different sides of the *x-axis*. We have the following Lemma (proof is omitted due to the space limitation).

Lemma 7 (Two-step Advance Lemma). *In a sensing-covered network, the projected progress in two consecutive steps on a BVGF routing path is more than Δ_2, where $\Delta_2 = \sqrt{R_c^2 - 4R_s^2}$.*

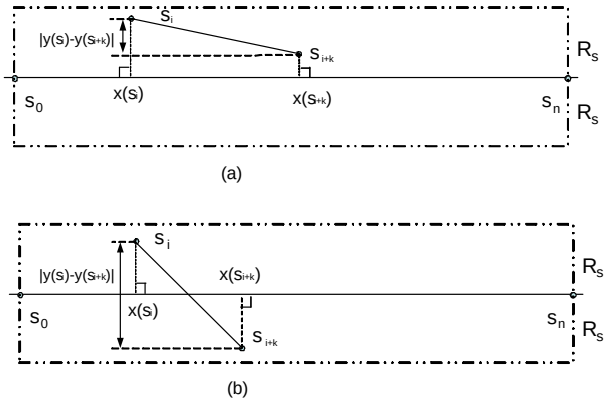

Figure 8: Projected Progress of Two Non-adjacent Nodes

Combining the different cases of non-adjacent node locations, we can derive the lower bound on the projected progress made by BVGF in four consecutive steps.

Lemma 8 (Four-step Advance Lemma). *In a sensing-covered network, the projected progress in four consecutive steps of a BVGF routing path is more than Δ_4, where*

$$\Delta_4 = \begin{cases} \sqrt{R_c^2 - R_s^2} & (2 \le R_c/R_s \le \sqrt{5}) \\ \sqrt{4R_c^2 - 16R_s^2} & (R_c/R_s > \sqrt{5}) \end{cases}$$

Proof. Let $s_0(u)$,$s_1 \cdots s_{n-1}$,$s_n(v)$ be the consecutive nodes on the BVGF routing path between source u and destination v. s_i, s_{i+2} and s_{i+4} are three non-adjacent nodes on the path. Without loss of generality, let s_i lie above the *x-axis*. Fig. 9(a)(b)(c)(d) show all possible configurations of s_i, s_{i+2} and s_{i+4} (the dotted boxes denote the Voronoi forwarding rectangles). We now derive the lower bound on the projected progress between s_i and s_{i+4}.

1).When s_i and s_{i+4} lie on different sides of the *x-axis*, as illustrated in Fig. 9(a)(b), the projected progress δ_{ab} between s_i and s_{i+4} is the sum of the projected progress between s_i and s_{i+2} and the projected progress between s_{i+2} and s_{i+4}. From Lemmas 6 :

$$\delta_{ab} = \sqrt{R_c^2 - R_s^2} + \sqrt{R_c^2 - 4R_s^2}$$

2).When s_i and s_{i+4} lie on the same side of the *x-axis*, as shown in Fig. 9(c)(d), from Lemma 6, the projected progress between them is more than $\delta_{cd} = \sqrt{R_c^2 - R_s^2}$. On the other hand, the projected progress can be computed as the sum of the projected progress between s_i and s_{i+2} and the projected progress between s_{i+2} and s_{i+4}, *i.e.*, $\delta_c = 2\sqrt{R_c^2 - 4R_s^2}$ as shown

in Fig. 9(c) or $\delta_d = 2\sqrt{R_c^2 - R_s^2}$ as shown in Fig. 9(d). Since $\delta_d > \delta_c$, the $\max\{\delta_{cd}, \delta_c\}$ is the lower bound on the projected progress between s_i and s_{i+4} when they lie on the same side of the *x-axis*.

Summarizing the cases 1) and 2), the lower bound on the projected progress in four consecutive steps on a BVGF routing path is

$$\Delta_4 = \min\{\delta_{ab}, \max\{\delta_{cd}, \delta_c\}\}$$

From the relation between δ_{ab}, δ_{cd} and δ_c, Δ_4 can be transformed to the result of the theorem. □

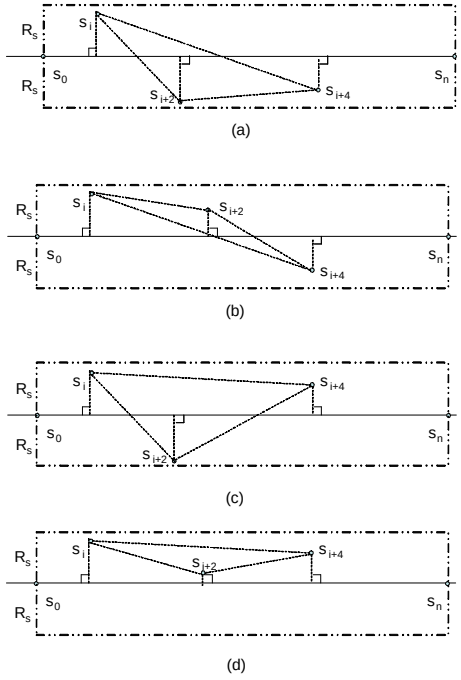

Figure 9: Projected Progress in Four Consecutive Steps

When R_c/R_s is small, the network is relatively sparse. Although the one-step projected progress approaches zero as shown in Lemma 4 in such a case, interestingly, Lemmas 7 and 8 show that the projected progress toward the destination made by BVGF in two or four consecutive steps is lower-bounded. On the other hand, when $R_c \gg R_s$, the sensing coverage of the network can result in a high density of nodes in the communication range of a routing node and hence the projected progress of BVGF in each step approaches R_c. In such a case the lower bound established in Lemma 4 is tighter than the lower bounds established in Lemmas 7-8.

Using Lemmas 4, 7 and 8, we now derive the upper bound on the network length of the BVGF routing path between any two nodes in a sensing-covered network.

Theorem 6. *In a sensing-covered network, The BVGF routing path between any two nodes u and v is no longer than Δ hops, where* $\Delta = \min\left\{\left\lceil \frac{|uv|}{\Delta_1} \right\rceil, 2\left\lfloor \frac{|uv|}{\Delta_2} \right\rfloor + 1, 4\left\lfloor \frac{|uv|}{\Delta_4} \right\rfloor + 3\right\}$.

Proof. Let N be network length of the BVGF routing path between nodes u and v. From Lemmas 4, 7 and 8, we have

$$N \leq \left\lceil \frac{|uv|}{\Delta_1} \right\rceil \quad (10)$$

$$N \leq 2\left\lfloor \frac{|uv|}{\Delta_2} \right\rfloor + 1 \quad (11)$$

$$N \leq 4\left\lfloor \frac{|uv|}{\Delta_4} \right\rfloor + 3 \quad (12)$$

From (10)-(12), we have

$$N \leq \min\left\{\left\lceil \frac{|uv|}{\Delta_1} \right\rceil, 2\left\lfloor \frac{|uv|}{\Delta_2} \right\rfloor + 1, 4\left\lfloor \frac{|uv|}{\Delta_4} \right\rfloor + 3\right\} \quad \square$$

From Theorem 6 and (1),the network dilation of a sensing-covered network $G(V, E)$ under BVGF satisfies:

$$D_n(BVGF) \leq \max_{u,v \in V} \frac{\Delta}{\left\lceil \frac{|uv|}{R_c} \right\rceil} \quad (13)$$

where Δ is defined in Theorem 6. The *asymptotic* bound on network dilation of sensing-covered networks under BVGF can be computed by ignoring the rounding and the constant terms in (13).

Theorem 7. *The asymptotic network dilation of a sensing-covered network under BVGF satisfies*

$$\tilde{D_n}(BVGF) \leq \begin{cases} \frac{4R_c}{\sqrt{R_c^2 - R_s^2}} & (2 \leq R_c/R_s \leq \sqrt{5}) \\ \frac{2R_c}{\sqrt{R_c^2 - 4R_s^2}} & (\sqrt{5} < R_c/R_s \leq 3.8) \\ \frac{R_c}{\sqrt{R_c^2 - 2R_cR_s} - R_s} & (R_c/R_s > 3.8) \end{cases}$$

7. Summary of Analysis on Network Dilations

In this section we summarize the network dilation bounds derived in previous sections. Fig. 10 shows the DT-based dilation bound and the asymptotic dilation bounds of GF and BVGF under different range ratios, as well as the simulation results that will be discussed in Section 8. The curve "BVGF Asymptotic Bound" shows the asymptotic bound on the network dilation of BVGF established in Theorem 7. We can

see the asymptotic bound of BVGF is competitive for all range ratios no smaller than two. The asymptotic bound of BVGF gets the worst-case value $\frac{8\sqrt{3}}{3} \approx 4.62$ when $R_c/R_s = 2$. That is, in a sensing-covered network that has the double range property, BVGF can always find a routing path between any two nodes u and v within $4.62 \left\lceil \frac{|uv|}{R_c} \right\rceil$ hops.

The asymptotic network dilation bound of GF increases quickly with the range ratio and approaches infinity when R_c/R_s is close to two. Whether there is a tighter bound for GF in such a case is an important open research question.

When $R_c/R_s >\sim 3.5$, the asymptotic network dilations of GF and BVGF are very similar because the network topology is denser and both algorithms can find very short routing paths. We can see the network dilation bound based on DT is significantly higher than the bounds of BVGF and GF when R_c/R_s becomes larger than ~ 2.5, because the analysis based on DT only considers DT edges (which have been shown to be shorter than $2R_s$ in Lemma 2) and becomes conservative when the communication range is much larger than the sensing range.

We should note that the network dilation of a sensing-covered network is upper-bounded by the minimum of the DT bound, the GF bound and the BVGF bound, because the network dilation is defined based on *shortest* paths.

8. Simulation Results

In this section we present our simulation results. The purpose of the simulations is twofold. First, we compare the network dilations of GF and BVGF routing algorithms under different range ratios. Second, we investigate the tightness of the theoretical bounds we established in previous sections.

The simulation is written in C++. There is no packet loss due to transmission collisions in our simulation environments. 1000 nodes are randomly distributed in a $500m \times 500m$ region. All simulations in this section are performed in sensing-covered network topologies produced by the Coverage Configuration Protocol (CCP) [33]. CCP maintains a set of active nodes to provide sensing coverage to the deployment region and redundant nodes are turned off for energy conservation. All nodes have the same sensing range of $20m$. We vary R_c to measure the network and Euclidean dilations of GF and BVGF under different range ratios. As discussed in Section 5, GF refers to two routing schemes, *i.e.*, a node chooses as the next hop a neighbor that has the shortest Euclidean or projected distance to the destination. Since the simulation results of the two schemes are very similar, only Euclidean distance based results are presented in this section.

The results presented in this section are averages of five runs on different network topologies produced by CCP. In each round, a packet is sent from each node to every other node in the network. As expected, 100% of the packets are delivered by both algorithms. The network and Euclidean lengths are logged for each communication. The network and Euclidean dilations are then computed using (1) and (2), respectively. To distinguish the dilations computed from the simulation results from the dilation bounds we derived in previous sections, we refer to the dilations obtained from the simulations as *measured dilations*. We should note that the measured dilations characterize the average-case performance of the routing algorithms in the particular network topologies used in our experiments, which may differ from the worst-case bounds for *any* possible sensing-covered network topologies we derived in previous sections.

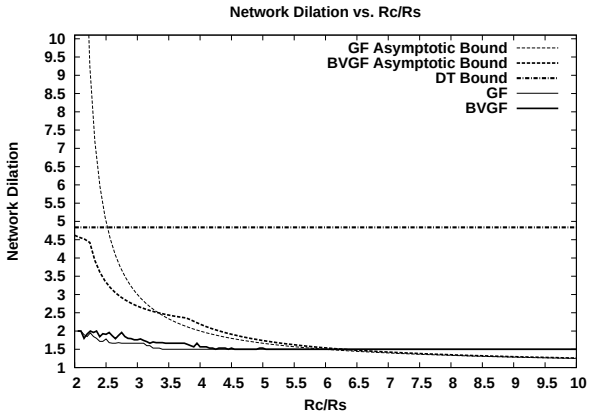

Figure 10: Network Dilations

From Fig. 10, we can see the measured dilations of GF and BVGF remain close to each other. Both GF and BVGF have very low dilations (smaller than two) in all range ratios no smaller than two. This result shows that both GF and BVGF can find short routing paths in sensing-covered networks. When R_c/R_s increases, the measured dilations of both algorithms approach their asymptotic bounds. When R_c/R_s is close to 2, however, the difference between the asymptotic bounds and the corresponding measurement becomes wider. This is because the measured dilations are obtained from the average-case network topologies and the worst-case scenarios from which the upper bounds on network dilations are derived are rare when the network is less dense.

Due to the rounding errors in deriving the asymptotic dilation bounds (Corollary 2 and Theorem 7), the measured network dilations are slightly higher than the asymptotic bounds for both algorithms when $R_c/R_s > 6$, as shown in Fig. 10. This is because when R_c becomes large, the routing paths chosen by both the algorithms become short and the effect of rounding in the calculation of network dilations becomes significant.

The result also indicates that the measured network dilation of GF is significantly lower than the asymptotic bound presented in this paper. Whether GF has a tighter network dilation bound is an open question that requires future work.

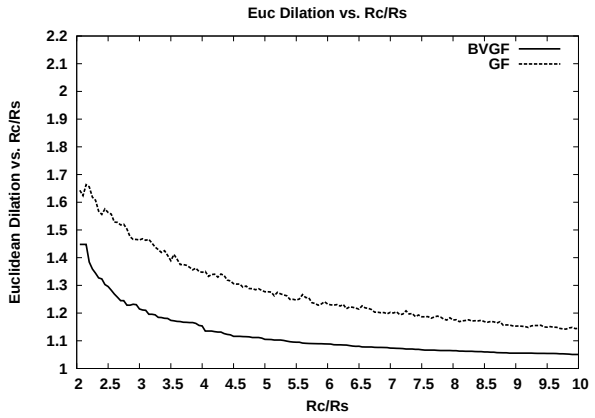

Figure 11: Euclidean Dilations

Fig. 11 shows the Euclidean dilations of GF and BVGF. BVGF outperforms GF for all range ratios. This is due to the fact BVGF always forwards a packet along a path inside the Voronoi forwarding rectangle. As mentioned in Section 3, the low Euclidean dilation may lead to potential energy savings in wireless communication.

The simulation results have shown that the proposed BVGF algorithm performs similarly with GF in average cases and has lower Euclidean dilation. In addition, the upper bounds on the network dilations of BVGF and GF established in previous sections are tight when R_c/R_s is large.

9. Conclusion

Our results lead to several important insights on the design of sensor networks. First, our analysis and simulation show that simple greedy geographic routing algorithms may be highly efficient in sensing-covered networks. Both the asymptotic bound and measured network dilations of BVGF and GF drop below 2.5 when the network's range ratio reaches 3.5. Moreover, the asymptotic network dilation bound of BVGF remains below 4.62 for any range ratio no smaller than 2. Our results also indicate that the redundant nodes can be turned off without significant increase in network length as long as the remaining active nodes maintain sensing coverage. Therefore, our analysis justifies coverage maintenance protocols [31, 33, 35] that conserve energy by scheduling nodes to sleep. Finally, our dilation bounds enable a source node to efficiently compute an upper-bound on the network length of its routing path based on the location of the destination. This capability can be useful to real-time communication protocols that require bounded routing paths to achieve predictable end-to-end communication delays.

In the future, we will generalize our analysis to sensing-covered networks without the double range property. Further analysis is also needed on the network dilations of GF when the range ratio approaches 2. Another important research area is to extend our analysis to handle probabilistic sensing and communication models.

References

[1] F. Aurenhammer. Voronoi diagrams -a survey of a fundamental geometric data structure. *ACM Computing Surveys*, 23(3):345–405, 1991.

[2] Bose and Morin. Online routing in triangulations. In *ISAAC: 10th International Symposium on Algorithms and Computation*, 1999.

[3] P. Bose, P. Morin, I. Stojmenovic, and J. Urrutia. Routing with guaranteed delivery in ad hoc wireless networks. *Wireless Networks*, 7(6):609–616, 2001.

[4] J. Broch, D. A. Maltz, D. B. Johnson, Y.-C. Hu, and J. Jetcheva. A performance comparison of multi-hop wireless ad hoc network routing protocols. In *Mobile Computing and Networking*, pages 85–97, 1998.

[5] K. Chakrabarty, S. S. Iyengar, H. Qi, and E. Cho. Grid coverage for surveillance and target location in distributed sensor networks. *IEEE Transactions on Computers*, 51(12):1448–1453, December 2002.

[6] L. Chew. There is a planar graph almost as good as the complete graph. In *In Proceedings of the 2nd Annual ACM Symposium on Computional Geometry*, pages 169–177, 1986.

[7] T. Couqueur, V. Phipatanasuphorn, P. Ramanathan, and K. K. Saluja. Sensor deployment strategy for target detection. In *Proceeding of The First ACM International Workshop on Wireless Sensor Networks and Applications*, pages 169–177, Sep 2002.

[8] Crossbow. Mica wireless measurement system datasheet. 2003.

[9] Crossbow. Mica2 wireless measurement system datasheet. 2003.

[10] D.P.Dobkin, S.J.Friedman, and K.J.Supowit. Delaunay graphs are almost as good as complete graphs. *Discrete and Computational Geometry*, 1990.

[11] M. Duarte and Y.-H. Hu. Distance based decision fusion in a distributed wireless sensor network. In *The 2nd International Workshop on Information Processing in Sensor Networks (IPSN 2003)*, Palo Alto,CA, April 22-23 2003.

[12] D. Eppstein. Spanning trees and spanners. Technical Report ICS-TR-96-16, 1996.

[13] G. Finn. Routing and addressing problems in large metropolitan-scale internetworks. Technical Report ISI Research Report ISU/RR-87-180, Inst. for Scientific Information, Mar, 1987.

[14] J. Gao, L. J. Guibas, J. Hershberger, L. Zhang, and A. Zhu. Geometric spanner for routing in mobile networks. In *Proc. 2nd ACM Symp. Mobile Ad Hoc Networking and Computing (MobiHoc'01)*, pages 45–55, Oct. 2001.

[15] G. L. Goodman. Detection and classification for unattended ground sensors. In R. Evans, L. White, D. McMichael, and L. Sciacca, editors, *Proceedings of Information Decision and Control 99*, pages 419–424, Adelaide, Australia, February 1999. Institute of Electrical and Electronic Engineers, Inc.

[16] J.M.Keil and C.A.Gutwin. Classes of graphs which approximate the complete euclidean graph. *Discrete Computational Geometry*, 7, 1992.

[17] B. Karp and H. T. Kung. GPSR: greedy perimeter stateless routing for wireless networks. In *Mobile Computing and Networking*, pages 243–254, 2000.

[18] F. Kuhn, R. Wattenhofer, and A. Zollinger. Worst-Case Optimal and Average-Case Efficient Geometric Ad-Hoc Routing. In *Proc. 4^{th} ACM Int. Symposium on Mobile Ad-Hoc Networking and Computing (MobiHoc)*, 2003.

[19] D. Li, K. Wong, Y. H. Hu, and A. Sayeed. Detection, classification and tracking of targets in distributed sensor networks. *IEEE Signal Processing Magazine*, 19(2), Mar. 2002.

[20] J. Li, J. Jannotti, D. De Couto, D. Karger, and R. Morris. A scalable location service for geographic ad-hoc routing. In *Proceedings of the 6th ACM International Conference on Mobile Computing and Networking (MobiCom '00)*, pages 120–130, Aug. 2000.

[21] X.-Y. Li, G. Calinescu, and P.-J. Wan. Distributed construction of a planar spanner and routing for ad hoc wireless networks, June 2002.

[22] M. Mauve, J. Widmer, and H. Hartenstein. A survey on position-based routing in mobile ad hoc networks, 2001.

[23] S. Meguerdichian, F. Koushanfar, M. Potkonjak, and M. B. Srivastava. Coverage problems in wireless ad-hoc sensor networks. In *INFOCOM*, pages 1380–1387, 2001.

[24] S. Meguerdichian and M. Potkonjak. Low power 0/1 coverage and scheduling techniques in sensor networks. Technical Report Technical Reports 030001, January 2003.

[25] R. Ramanathan and R. Hain. Topology control of multihop wireless networks using transmit power adjustment. In *INFOCOM (2)*, pages 404–413, 2000.

[26] S. Ramanathan and M. Steenstrup. A survey of routing techniques for mobile communications networks. *Mobile Networks and Applications*, 1(2):89–104, 1996.

[27] Sensoria. sgate datasheet. 2003.

[28] SonicWall. Long range wireless card datasheet. 2003.

[29] I. Stojmenovic and X. Lin. Loop-free hybrid single-path/flooding routing algorithms with guaranteed delivery for wireless networks. *IEEE Transactions on Parallel and Distributed Systems*, 12(10):1023–1032, 2001.

[30] H. Takagi and L. Kleinrock. Optimal transmission ranges for randomly distributed packet radio terminals. *IEEE Transactions on Communications*, 32(3):246–257, 1984.

[31] D. Tian and N. Georganas. A coverage-preserved node scheduling scheme for large wireless sensor networks. In *Proceedings of First International Workshop on Wireless Sensor Networks and Applications (WSNA'02)*, pages 169–177, Atlanta, USA, Sep 2002.

[32] P. Varshney. *Distributed Detection and Data Fusion*. Spinger-Verlag, New York, NY, 1996.

[33] X. Wang, G. Xing, Y. Zhang, C. Lu, R. Pless, and C. D. Gill. Integrated coverage and connectivity configuration in wireless sensor networks. In *The First ACM Conference on Embedded Networked Sensor Systems(Sensys 03)*, 2003.

[34] R. Wattenhofer, L. Li, P. Bahl, and Y.-M. Wang. Distributed topology control for wireless multihop ad-hoc networks. In *INFOCOM*, pages 1388–1397, 2001.

[35] F. Ye, G. Zhong, S. Lu, and L. Zhang. Peas: A robust energy conserving protocol for long-lived sensor networks. In *The 23rd International Conference on Distributed Computing Systems (ICDCS'03)*, pages 169–177, May 2003.

[36] J. Zhao and R. Govindan. Understanding packet delivery performance in dense wireless sensor networks. In *The First ACM Conference on Embedded Networked Sensor Systems(Sensys 2003)*, Los Angeles, CA, November 2003.